JCSE The Journal of Corrosion Science and Engineering
ISSN 1466-8858 Volume 13, Preprint 53 submitted 16 December 2010

Influence of Temperature on Anti-sulfur Steels in simulated Oilfield Solution with High CO_2/H_2S Corrosion

Z.F. Yin [a,*], X.Z. Wang[a], S.D. Zhu[b] and C.X. Yin[c]

[a] Petroleum Research Institute, Shaanxi Yanchang Petroleum Group Company, Xi'an 710075, P.R. China

[b] School of Materials Science and Engineering, Xi'an Jiaotong University, Xi'an 710049, P.R. China

[c]The Key Laboratory for Mechanical and Environmental Behavior of Tubular Goods, Tubular Goods Research Center, CNPC, Xi'an 710065, P.R. China

Abstract

The present work investigated the influence of temperature on the characterization of corrosion product films and corrosion rates of anti-sulfur steels in the H_2S/CO_2 containing oilfield environment at various temperatures. The resistance of anti-sulfur steels to CO_2/H_2S corrosion was highlighted to provide information for material selection in sour corrosion oilfield. The corrosion rates were calculated by weight loss method carried out in the high-temperature and high-pressure autoclave. Meanwhile, surface morphologies of corrosion product films were studied by means of scanning electron microscopy (SEM) with energy dispersive spectrometry (EDS). The results indicated that the corrosion product films became more protective and the corrosion rates of anti-sulfur steels substantially decreased with increasing temperature. H_2S corrosion dominated the corrosion process under the test conditions. In addition, the anti-sulfur materials of both P110S and N80SS were superior to the common steel P110 in the CO_2/H_2S corrosion environment especially at temperature below 120 ^oC.

Keywords: Anti-sulfur steels, CO_2/H_2S corrosion, Temperature, Corrosion product film

* Corresponding author: yinzhifu919@sohu.com (Z.F. Yin)

JCSE The Journal of Corrosion Science and Engineering
ISSN 1466-8858 Volume 13, Preprint 53 submitted 16 December 2010

1 Introduction

The corrosion environments containing CO_2 and H_2S greatly exist in oil and gas industry, which has aroused considerable attentions among the academic community in past several decades [1-4]. Compared to the pure CO_2 corrosion, the sour corrosion with H_2S was primarily focused on the aspects such as various corrosion products of ferric sulfide, H_2S concentration, corrosion environments with various pH values and thermodynamic and kinetic models. Especially the multiphase types of ferric sulfides such as Mackinawite, Troilite, Pyrrhotite and Pyrite in corrosion product films were extensively reported in the open literatures [5-8]. The combined presence of CO_2 and H_2S acidic gases modifies the corrosion mechanisms and characteristics significantly with respect to that caused by sole CO_2 or H_2S.

The effect of temperature is one of most important influence factors, which has been studied to capture more information of material degradation process. The corrosion rate tests with CO_2 and H_2S or without H_2S were conducted on carbon steel in the temperature ranges of 25 ^oC to 90 ^oC, the PH value ranged from 3.85 to 4.15 in a flow loop [9]. In the environments of various H_2S concentrations at temperatures ranged from 30 ^oC to 90 ^oC, the evaluation indicated that the sulphide stress corrosion cracking was less pronounced at higher temperature due to the protective corrosion product films formation [10]. Three flow loop corrosion experiments of carbon steel exposed to synthetic produced water for 2-3 weeks under simulated Kashagan field conditions were conducted at temperatures 25 ^oC and 80 ^oC, flow velocities 1-5 m/s, H_2S partial pressures of 10 and 30 bar, CO_2 partial pressures of 3.3 and 10 bar and a H_2S/CO_2 ratio of 3 [11]. The result indicated that the average corrosion rates were in the range of 0.5-1.5 mm/y for all experiments, and did not vary much with temperature. These corrosion rates are substantially

ISSN 1466-8858 Volume 13, Preprint 53 submitted 16 December 2010

lower than corrosion rates observed in systems with similar conditions without H_2S. Lab tests were performed to determine corrosion rate of carbon steel at temperatures ranged from 50 ^oC to 150 ^oC under a total pressure of 3.27 MPa CO_2 with trace of H_2S, which presented that temperature has influence on H_2S solubility as well as the stability of corrosion films [12]. In addition, the corrosion of carbon steel and the effect of surface films in a CO_2-H_2S-H_2O system were studied in the temperature range of 50 ^oC to 90 ^oC using mass loss [13]. It suggested that the corrosion rates increased with temperature.

In the past studies, these authors carried out a series of corrosion experiments as a function of temperature. The experiments were related with various test conditions consisting of the temperature range, gas pressure, pH value, exposure time and the simulated solution, which led to the confusing and incompatible experimental data for understanding of corrosion mechanisms. However, these reports related with the anti-sulfur materials in high CO_2/H_2S corrosion were very few. In this work, the aim was to investigate the effect of temperature on the anti-sulfur steels of P110S and N80SS as compared to the common P110 steel at the temperature ranges of 90 ^oC to 180 ^oC in the high CO_2/H_2S containing environment.

2 Experimental

2.1 Materials preparation

The samples of P110, P110S and N80SS were processed into steel slices with a size of 35×25×3 mm, whose chemical compositions were listed in Table 1. The samples were initially polished by emery sandpaper progressively up to 800 grit, then degreased with acetone and rinsed with absolute alcohol, weighted using an electronic balance with a precision of 0.1 mg, finally put in the high-temperature and high-pressure autoclave made by Cortest (in USA).

JCSE The Journal of Corrosion Science and Engineering
ISSN 1466-8858 Volume 13, Preprint 53 submitted 16 December 2010

Table 1 The chemical compositions of P110, P110S and N80SS steels (wt.%)

Materials	C	Mn	Si	P	S	Cr	Mo	Ni	V	Ti
P110	0.26	1.40	0.20	0.009	0.003	0.15	0.01	0.012	0.012	0.03
P110S	0.26	1.02	0.25	0.012	0.0026	0.62	0.017	0.032	0.006	0.008
N80SS	0.26	0.45	0.23	0.007	0.006	1.02	0.31	0.032	0.006	0.024

2.2 Weight loss measurements

The test solution was composed of deionized water and pure chemical agents with the ions concentrations of 8.5 g/L Cl^-, 4.2 g/L HCO_3^-, 0.5 g/L SO_4^{2-}, 0.4 g/L Ca^{2+}, 0.08 Mg^{2+} and 1.1 g/L (K^++Na^+). Prior to the weight loss tests, the solution was deoxygenated with bubbling the pure N_2 for 12 h before the introduction of CO_2 (600 psi) and H_2S (50 psi), and then the solution in the autoclave was pressured with pure N_2 gas to the total pressure value of 1200 psi. Experiments were performed in the temperature ranges 90 ^oC~180 ^oC. All tests were carried out for 120 h under dynamic condition with a rotational speed of 400 r/min. At least three samples were tested for each experimental condition. After each test the samples were rinsed with distilled water and ethanol, and then they were divided into two groups: the samples in group one were descaled with Clark solution (20 g Sb_2O_3 + 50 g $SnCl_2$ + 1 L HCl), then the visual observation was done and the weight loss was measured.

2.3 SEM and EDS analysis

The samples with corrosion product films in group two were not descaled, which were dried and stored in desiccator. Then, the surface morphologies were performed by using scanning electron microscopy (SEM), and the energy dispersive spectrometry (EDS) was utilized to analyze the element contents of corrosion product films.

JCSE The Journal of Corrosion Science and Engineering
ISSN 1466-8858 Volume 13, Preprint 53 submitted 16 December 2010

3 Results and discussion

3.1 SEM observation

Figure 1 presents the surface morphologies of corrosion product films on P110 steels exposed in the CO_2/H_2S corrosion environment at temperatures of 90 ^oC, 120 ^oC 150 ^oC and 180 ^oC, respectively. It is clear that the localized corrosion occurs at multiple sites of sample surface at 90 ^oC, as temperature increases the corrosion product films cover the whole steel surfaces and the crystal size becomes more obvious and larger. The corrosion product films can be protective or non-protective, which is dependent on the compactness and solubility of the corrosion products. Simultaneously, the protectivity of corrosion product films can be identified by corrosion rate. It is worth noting that at 150 ^oC, massive breakdown of corrosion films can be due to the test performed under turbulent flow condition and the occurrence of internal stress in the presence of H_2S. The naked steel then continues to react with the corrosive species in the bulk solution, leading to further material degradation. However, if the corrosion films are non-protective layer which can not inhibit the diffusion transport of ferrous ion and the anions through the aqueous phase in spite of the films can completely cover the steel surface, the anodic dissolution of steel will increase the corrosion rate.

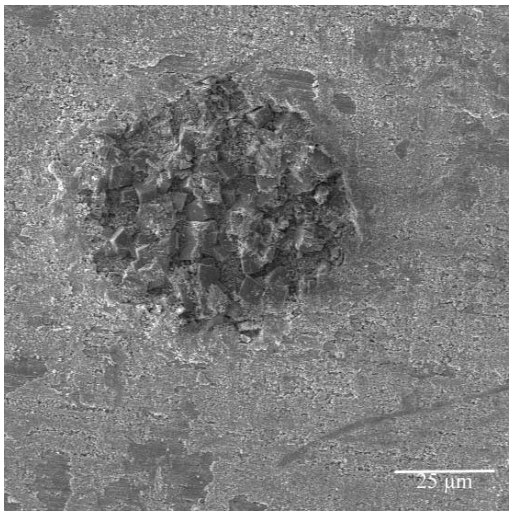

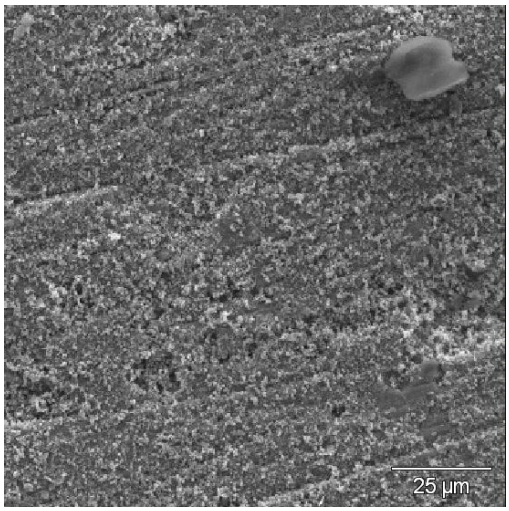

JCSE The Journal of Corrosion Science and Engineering
ISSN 1466-8858 Volume 13, Preprint 53 submitted 16 December 2010

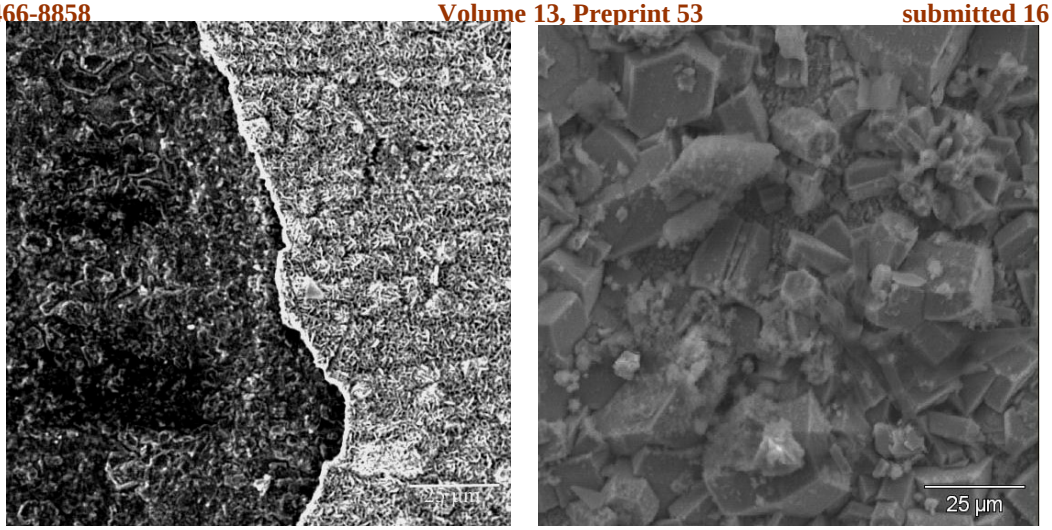

Figure 1 SEM images of the corrosion product films of P110 steel exposed in the CO_2/H_2S corrosion environment at various temperatures (a) 90 ^oC, (b) 120 ^oC, (c) 150 ^oC and (d) 180 ^oC.

Compared with the SEM images in Fig. 1, the surface morphologies of anti-sulfur steels of P110S and N80SS have similar structure characteristics of corrosion product films at the corresponding temperatures as shown in Figs. 2 and 3. After the initial corrosion film formation, the corrosion species can discontinuously reach the steel surface due to the corrosion film acts as a barrier to a certain extent. Therefore, the discontinuous penetration of relatively massive corrosion product through the initial corrosion film results in the deposition of partial corrosion product underlying the initial film, finally the partial film breaks down due to the stress generation. In the cases of films breakdown, we can find that there is a layer of compact and protective thin film precipitates close to the bare steels at the sites where the massive film are peeled away. It is considered that the iron sulfide corrosion product can preferentially form based on the film breakdown phenomenon and the fact [14] that H_2S gas is about three times more soluble in aqueous solution than CO_2 gas. In addition, the great crystal grains of iron carbonate at 180 ^oC can be observed in Fig. 2d and 3d, which will be further confirmed by EDS as follows.

JCSE The Journal of Corrosion Science and Engineering
ISSN 1466-8858 Volume 13, Preprint 53 submitted 16 December 2010

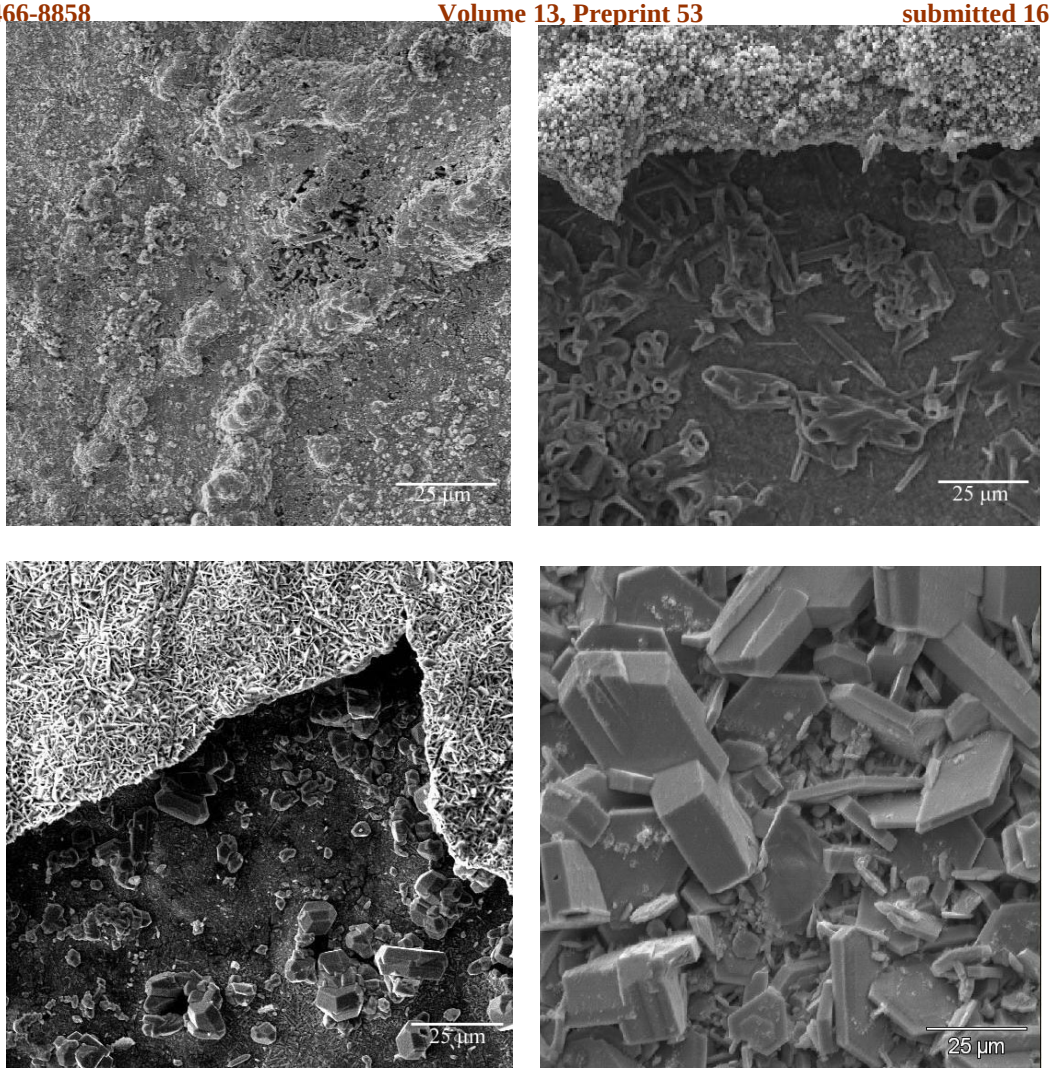

Figure 2 SEM images of the corrosion product films of anti-sulfur P110S steel exposed in the CO_2/H_2S corrosion environment at various temperatures (a) 90 ^oC, (b) 120 ^oC, (c) 150 ^oC and (d) 180 ^oC.

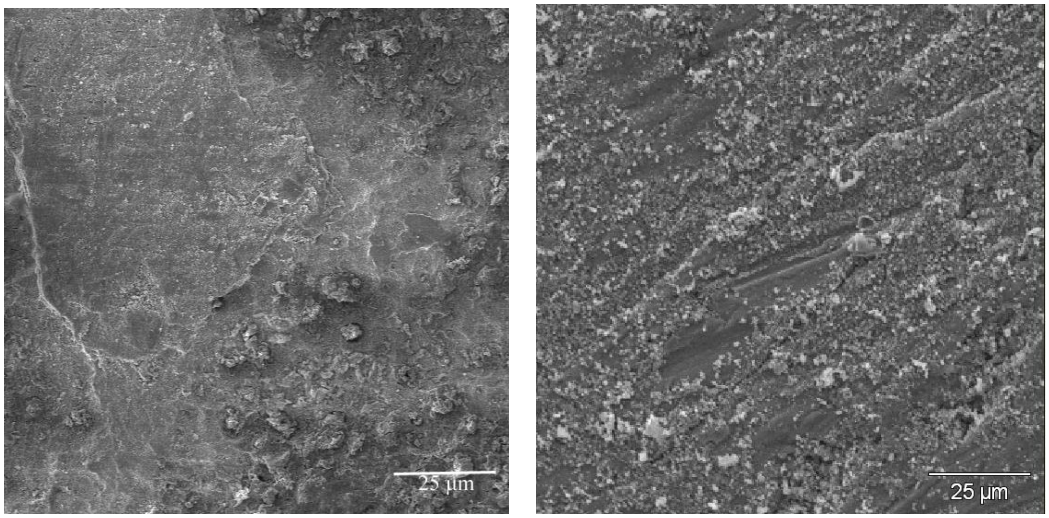

JCSE The Journal of Corrosion Science and Engineering
ISSN 1466-8858 Volume 13, Preprint 53 submitted 16 December 2010

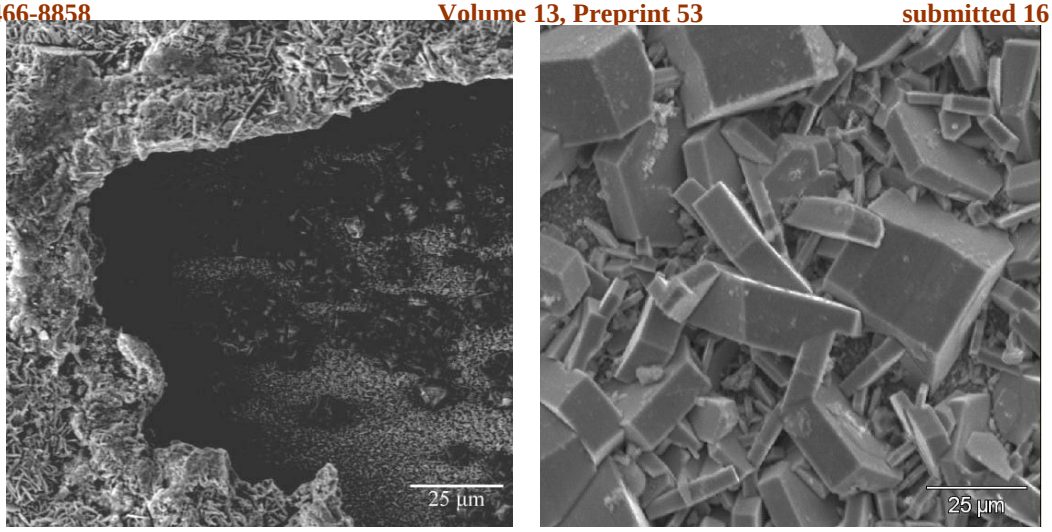

Figure 3 SEM images of the corrosion product films of anti-sulfur N80SS steel exposed in the CO_2/H_2S corrosion environment at various temperatures (a) 90 °C, (b) 120 °C, (c) 150 °C and (d) 180 °C.

3.2 EDS analysis

The energy dispersive spectrometry (EDS) can provide much information on the corrosion product films exposed in the CO_2/H_2S corrosion environment. Figure 4 shows the Fe/S (at.%) ratio of the corrosion product films of P110, P110S and N80SS steels exposed at various temperatures. From the detected data, it can be seen that the Fe/S (at.%) ratio first increases and then decrease and finally increases again, which indicates that the product type of iron sulfide changes with temperature. Obviously, all Fe/S (at.%) ratios are almost greater than 1 which suggests that the corrosion products are FeS or FeS_{1-X} (rich-iron type) in addition to the presence of iron carbonate ($FeCO_3$) in some conditions. In the study related with partial pressure ratio CO_2/H_2S [15], they considered that when the ratio is $20 < CO_2/H_2S < 500$, both CO_2 corrosion and H_2S corrosion jointly dominate the corrosion process and a mixture of FeS and $FeCO_3$ are the main corrosion products. Moreover, according to the EDS data, we found that the elements of carbon and oxygen existed in the corrosion product films only detected at 180 °C. Figure 4 only presents the EDS

spectra of the corrosion product films of P110S steels exposed in the CO_2/H_2S corrosion environment at 120 ^oC and 180 ^oC. In fact, the three materials have similar element characteristics at corresponding temperatures. It can conclude that trace of corrosion product of iron carbonate exists in the corrosion films at higher temperature in this test conditions. At the same time, it is also indicates that the products of both FeS and $FeCO_3$ exist the competitive kinetics of precipitation.

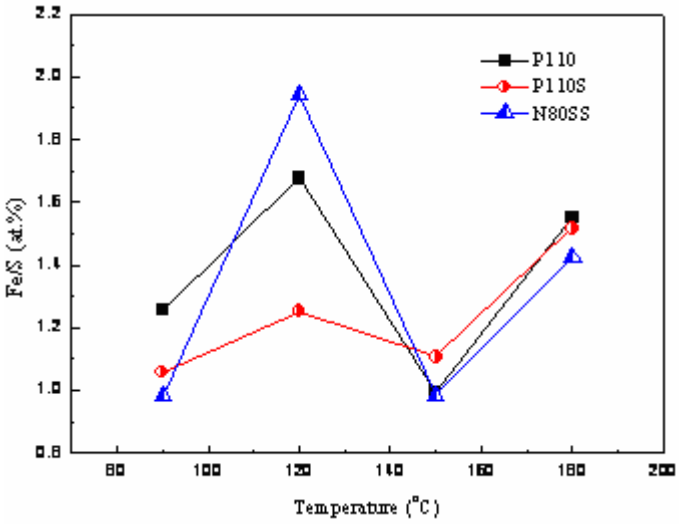

Figure 4 Fe/S (at.%) of the corrosion product films of P110, P110S and N80SS steels exposed in the CO_2/H_2S corrosion environment at various temperatures.

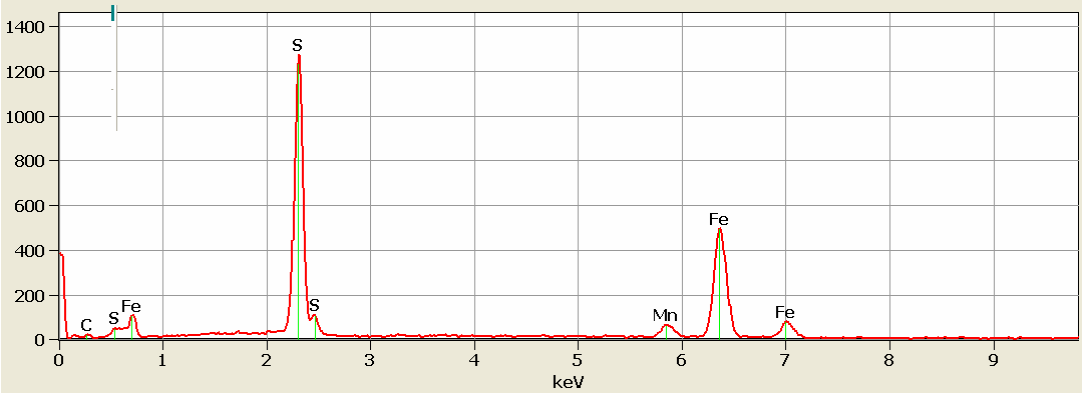

JCSE The Journal of Corrosion Science and Engineering
ISSN 1466-8858 Volume 13, Preprint 53 submitted 16 December 2010

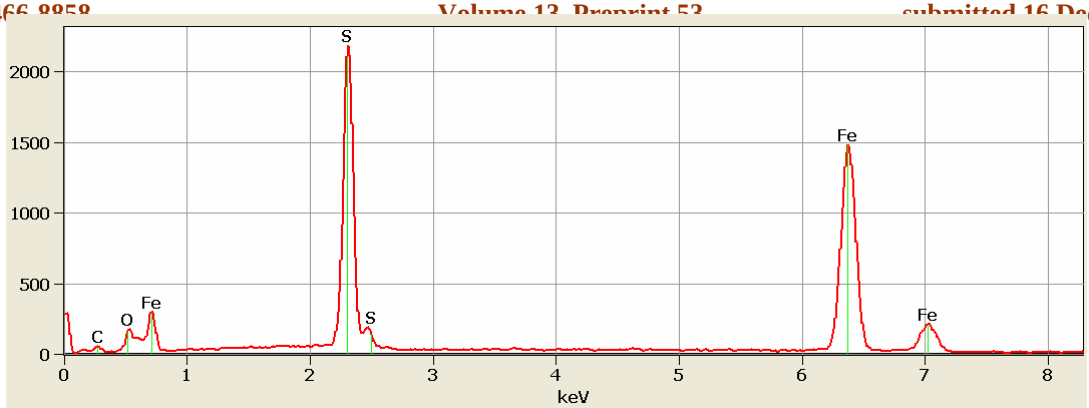

Figure 5 The EDS spectra of the corrosion product films of P110S steels exposed in the CO_2/H_2S corrosion environment at temperatures: (a) 120 ^oC and (b) 180 ^oC.

3.3 Corrosion rate calculation

Figure 6 shows the corrosion rate of P110, P110S and N80SS steels exposed in the CO_2/H_2S corrosion environment at various temperatures. It is clear that the corrosion rates of three test materials almost decrease with increasing temperature. The differences of corrosion rates among three test materials gradually reduce as temperature increases, which can be due to formation of the protective corrosion films. The corrosion is effectively mitigated with further evolvement of the protective films as temperature increases. According to the investigation under the conditions of both partial pressure ratio $CO_2H_2S < 200$ and temperature ranging from 60 ^oC to 240 ^oC [16], it was claimed that the protective films were initially mackinawite and then the more protective and stable corrosion product of pyrrhotite was formed at higher temperature. The result can provide proof for the result of the present tests. From the data in Fig. 6, we can estimate that the anti-sulfur materials of P110S and N80SS are superior to the common steel of P110 in the resistance to corrosion attack, especially at temperature lower than 120 ^oC. We think that the superiority of P110S and N80SS is attributed to the higher contents of Cr, Mo and Ni and lower Mn content in the chemical compositions, as shown in Table 1. Nevertheless, when temperature increases beyond

ISSN 1466-8858 Volume 13, Preprint 53 submitted 16 December 2010

the temperature of 150 °C, the corrosion rates of three materials almost keep the same values. The result is in accordance with the result of SEM observation, i.e., the steel surfaces form multi-layer of compact and dense corrosion films which can render greatly effective protection the bare steel underneath the protective films.

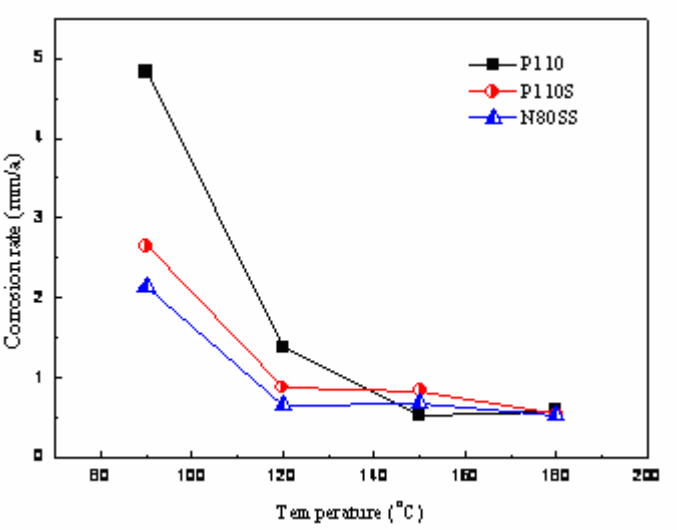

Figure 6 Corrosion rates of P110, P110S and N80SS steels exposed in the CO_2/H_2S corrosion environment at various temperatures.

3.4 Corrosion mechanisms

3.4.1 Effect of alloy elements

In Table 1, it can be seen that the alloy elements such as main alloy element of Cr, Ni, Mo, Mn, and the trace of Ti and V, which can promote the anti-corrosion performance except for Mn element. In general, Mn combined with S can form the inclusion of MnS, which serves as micro-cathode in steel and promotes local corrosion. Therefore, the content of Mn plays a negative role in CO_2/H_2S corrosion. Based on the data in Table 1, the content of Mn element with respect to P110, P110SS and N80SS are respectively 1.40%,1.02% and 0.45%, which contributes the anti-corrosion performance: P110 < P110SS < N80SS. The nickel (Ni), in conjunction with the molybdenum (Mo), also gives outstanding resistance to reducing environments such as those

ISSN 1466-8858 Volume 13, Preprint 53 submitted 16 December 2010

containing sulfuric acids. Chromium (Cr) also improves resistance to high-temperature oxidation and to attack by hot sulfur-bearing gases. Besides, the minor molybdenum (Mo) also increases resistance to pitting and crevice corrosion especially at high temperature [17]. It is obvious that the content of the alloy elements of Cr, Ni and Mo in anti-sulfur steels are much more than those in the common carbon steel.

3.4.2 Temperature and partial pressure ratio CO_2/H_2S

Temperature is one of the most important factors in oil and gas industries. In general, at low temperature, the corrosive species such as HS^-, HCO_3^- and Cl^- may more rapidly penetrate through the non-protective corrosion films to react with the bare steel below the films when temperature increases, which may activate and accelerate these species in thermodynamic and kinetic views. Beyond certain temperature, one layer of protective films can form and can effectively inhibit large amounts of solution species diffusion transformation between bulk solution and substrate surface. Therefore, corrosion rate substantially decreases up to almost constant when temperature further increases.

Partial pressure ratio CO_2/H_2S is always related with the studies in combined CO_2/H_2S corrosion environments [15,16,18]. The partial pressure ratio CO_2/H_2S is used to predict the probable corrosion mechanism or to the buildup of corrosion model. The authors [15] considered that at partial pressure ratio $20 < CO_2/H_2S < 500$, both CO_2 corrosion and H_2S corrosion in common dominate the corrosion process, while, at $CO_2/H_2S < 500$ and $CO_2/H_2S > 20$, corrosion process is respectively controlled by CO_2 corrosion and H_2S corrosion. In present work, the partial pressure ratio CO_2/H_2S equals to 12, which indicates the H_2S corrosion dominates the corrosion process. From the SEM and EDS discussion above, they are mutually identified. However, we

ISSN 1466-8858 Volume 13, Preprint 53 submitted 16 December 2010

think that for the estimation of prediction model or mechanism, the partial pressures of CO_2 and H_2S and the total pressure are also very significant factors besides considering the partial pressure ratio CO_2/H_2S. In present work, the great amounts of partial pressures of CO_2 and H_2S can greatly change corrosion rate, corrosion kinetics and corrosion products and so on.

3.4.3 Effect of corrosion product films

In fact, the whole corrosion process is dependent on corrosion product films. The porous and loose films can not act as an effective barrier leading to the severe attack. But, once the compact and protective film formation, the corrosion rate can obviously decrease. The effective protection of corrosion films is as a function of temperature, pressure, pH value, flow velocity and other factors. Nevertheless, all factors can gather to one key parameter that is so-called supersaturation exponent. The ferrous ion (Fe^{2+}) may diffuse into solution to form corrosion products $FeCO_3$ and/or FeS so long as $[Fe^{2+}] \times [CO_3^{2-}]$ and /or $[Fe^{2+}] \times [S^{2-}]$ exceed the solubility products (K_{sp}) of iron carbonate and/or iron sulfide, and corrosion products can precipitate on the steel surface. The corrosion product films can grow and some can nucleate and grow time and again. At some conditions, the corrosion product films can provide a layer of protective film which can decreases the corrosion rate. In some sites where localized corrosion happens, the breakdown of massive films can also induce the severe galvanic corrosion.

4 Conclusions

The anti-sulfur materials of both P110S and N80SS were superior to the common steel P110 in the combined CO_2/H_2S corrosion environment especially at temperature below 120 ^oC. The corrosion rates of three materials were almost close to constant at high temperature above 150 ^oC. The massive areas of surface films of three materials were cracked and peeled away. The compact

ISSN 1466-8858 Volume 13, Preprint 53 submitted 16 December 2010

and protective films formed at temperature above 150 ^{o}C. Trace of corrosion product of iron carbonate exists in the corrosion films at higher temperature besides the abundant iron sulfide. H_2S corrosion dominates the corrosion process at the partial pressure ratio CO_2/H_2S of 12 applied into the tests.

References

[1] “Corrosion of iron in an H_2S-CO_2-H_2O system mechanism of sulfide film formation and kinetics of corrosion reaction”, J.B. Sardisco, R.E. Pitts, *Corrosion*, **21**, 8, pp. 245-53, 1965.

[2] “CO_2/H_2S corrosion under wet gas pipeline conditions in the presence of bicarbonate chloride and oxygen”, F.F. Lyle, H.U. Schutt, *Corrosion*/98, Paper no. **11**, NACE, Houston, TX, 1998.

[3] “Simulation of CO_2/H_2S corrosion using thermodynamic and electrochemical models”, A. Anderko, R.D. Young, *Corrosion*/99, Paper no. **31**, NACE, Houston, TX, 1999.

[4] “Effect of CO HS on the composition and stability of passive film on iron alloys in geothermal water”, J. Banas, U. Lelek-Borkowska, B. Mazurkiewicz, W. Solarski, *Electrochimica Acta*, **52** 18, pp. 5704-14, 2007.

[5] “Nature of sulfides and their corrosive effect on ferrous metals: A review”, J.S. Smith, J.D.A. Miller, *British Corrosion Journal*, **10**, 3, pp. 136-43, 1975.

[6] “The formation of ferrous monosulfide polymorphs during the corrosion of iron by aqueous hydrogen sulfide at 2l^{o}C”, D.W. Shoesmith, P. Taylor, M.G. Bailey, D.G. Owen, *Journal of The Electrochemical Society*, **127**, 5, pp. 1007-15, 1980.

[7] “Electrochemical growth of iron sulfide films in H_2S-saturated chloride media”, H. Ledage, T.A. Ramanarayanan, J.D. Mumford, S.S. Smith, *Corrosion*, **49**, 2, pp. 114-21, 1993.

[8] “Corrosion and deposition during the exposure of carbon steel to hydrogen sulphide-water

solutions", A.G. Wikjord, T.E. Rummery, F.E. Doern, D.G. Owen , *Corrosion Science*, **20**, 5, pp. 651-71, 1980.

[9] "Flow loop studies of the relationship between limiting currents and CO_2/H_2S corrosion of carbon steel", J. Kvarekal, *Corrosion*/98, Paper No. **44**, NACE, Houston, TX, 1998.

[10] "Formation rates of protective iron sulfide films on mild steel in HS saturated brine as a function of temperature", W.H. Thomason, *Corrosion*/78, Paper no. **41**, NACE, Houston, TX, 1978.

[11] "H_2S corrosion of carbon steel under simulated kashagan field conditions", I.H. Omar, Y.M. Gunaltun, J. Kvarekval, A. Dugustad, *Corrosion*/05, Paper no. **300**, NACE, Houston, TX, 2005.

[12] "The effect of small amounts of H_2S on CO_2 corrosion of a carbon steel", A. Valdes, R. Case, M. Ramirez, A. Ruiz, *Corrosion*/98, Paper no. **22**, NACE, Houston, TX, 1998.

[13] "The effect of surface films on corrosion of carbon steel in a CO_2-H_2S-H_2O system", D. Abayarathna, A. Naraghi, S.H. Wang, *Corrosion*/05, Paper no. **624**, NACE, Houston, TX, 2005.

[14] "Materials design strategy: effect of H_2S/CO_2 corrosion on materials selection", B. Kermani, J. Martin, K. Esaklul, *Corrosion*/06, Paper no. **121**, NACE, Houston, TX, 2006.

[15] "Improvements of de Waard-Willians corrosion prediction and applications to corrosion management", F.M. Pots, R.C. John, I.J. Rippon, M.J.J. Simon Thomas, S.D.Kapusta, M.M. Girgis, T. Whiteamn, *Corrosion*/02, Paper no. **235**, NACE, Houston, TX, 2002.

[16] "Prediction of corrosivity of CO_2/H_2S production environments", S. Srinivasan, R.D. Kane, *Corrosion*/96, Paper no. **11**, NACE, Houston, TX, 1996.

[17] D.C. Agarwal, J. Kloewer, "Ni-base alloys: corrosion challenges in the new millennium", *Corrosion*/01, Paper no. **325**, NACE, Houston, TX, 2001.

ISSN 1466-8858 Volume 13, Preprint 53 submitted 16 December 2010

[18] “Corrosion prediction and materials selection for oil and gas production environments”, L. Smith, K. de Waard, *Corrosion*/01, Paper no. **648**, NACE, Houston, TX, 2005.